The CMS di-photon excess at 95 GeV in view of the LHC Run 2 results

Thomas Biekötter [a],[*], Sven Heinemeyer [b], Georg Weiglein [c],[d]

[a] *Institute for Theoretical Physics, Karlsruhe Institute of Technology, Wolfgang-Gaede-Str. 1, 76131 Karlsruhe, Germany*
[b] *Instituto de Física Teórica UAM-CSIC, Cantoblanco, 28049, Madrid, Spain*
[c] *Deutsches Elektronen-Synchrotron DESY, Notkestr. 85, 22607 Hamburg, Germany*
[d] *II. Institut für Theoretische Physik, Universität Hamburg, Luruper Chaussee 149, 22607 Hamburg, Germany*

ARTICLE INFO

ABSTRACT

The CMS collaboration has recently reported the results of a low-mass Higgs-boson search in the di-photon final state based on the full Run 2 data set with refined analysis techniques. The new results show an excess of events at a mass of about 95 GeV with a local significance of $2.9\,\sigma$, confirming a previously reported excess at about the same mass and similar significance based on the first-year Run 2 plus Run 1 data. The observed excess is compatible with the limits obtained in the corresponding ATLAS searches. In this work, we discuss the di-photon excess and show that it can be interpreted as the lightest Higgs boson in the Two-Higgs doublet model that is extended by a complex singlet (S2HDM) of Yukawa types II and IV. We show that the second-lightest Higgs boson is in good agreement with the current LHC Higgs-boson measurements of the state at 125 GeV, and that the full scalar sector is compatible with all theoretical and experimental constraints. Furthermore, we discuss the di-photon excess in conjunction with an excess in the $b\bar{b}$ final state observed at LEP and an excess observed by CMS in the di-tau final state, which were found at comparable masses with local significances of about 2σ and 3σ, respectively. We find that the $b\bar{b}$ excess can be well described together with the di-photon excess in both types of the S2HDM. However, the di-tau excess can only be accommodated at the level of 1σ in type IV. We also comment on the compatibility with supersymmetric scenarios and other extended Higgs sectors, and we discuss how the potential signal can be further analyzed at the LHC and at future e^+e^- colliders.

© 2023 The Author(s). Published by Elsevier B.V. This is an open access article under the CC BY license (http://creativecommons.org/licenses/by/4.0/). Funded by SCOAP³.

1. Introduction

In the year 2012 the ATLAS and CMS collaborations discovered a new particle [1,2]. Within the current experimental and theoretical uncertainties the properties of the observed particle are consistent with the predictions for the Higgs boson of the Standard Model (SM) with a mass of approximately 125 GeV [3,4], but they are also compatible with many scenarios of physics beyond the SM (BSM). While the minimal scalar sector of the SM features only one physical scalar particle, BSM physics often gives rise to extended Higgs sectors in which additional scalar particles are present. Accordingly, one of the primary objectives of the LHC is the search for additional Higgs bosons, which is of crucial importance for exploring the underlying physics of electroweak symmetry breaking.

Searches for Higgs bosons below 125 GeV have been performed at LEP [5–7], the Tevatron [8] and the LHC [9–15]. Among them, searches for di-photon resonances are particularly intriguing, as

this decay mode constituted one of the two discovery channels of the Higgs boson at 125 GeV. CMS has performed searches for scalar di-photon resonances at 8 TeV and 13 TeV. Results based on the 8 TeV data and the first year of Run 2 data at 13 TeV, corresponding to an integrated luminosity of $19.7\,\mathrm{fb}^{-1}$ and $35.9\,\mathrm{fb}^{-1}$, respectively, showed a local excess of $2.8\,\sigma$ at 95.3 GeV [9,10]. This excess, which is present in both the 8 TeV and the 13 TeV data set, received considerable attention already soon after it was made public, see e.g. Refs. [16–26].

Recently, CMS published the result based on their full Run 2 data set and with substantially refined analysis techniques. This new analysis confirmed the excess of di-photon events at about 95 GeV [15]. By combining the data from the first, second, and third years of Run 2, which were collected at 13 TeV and correspond to integrated luminosities of $36.3\,\mathrm{fb}^{-1}$, $41.5\,\mathrm{fb}^{-1}$ and $54.4\,\mathrm{fb}^{-1}$, respectively, CMS finds an excess with a local significance of $2.9\,\sigma$ at a mass of 95.4 GeV. This "di-photon excess" can be described by a scalar resonance with a signal strength of [27]

$$\mu_{\gamma\gamma}^{\mathrm{exp}} = \frac{\sigma^{\mathrm{exp}}\left(gg \to \phi \to \gamma\gamma\right)}{\sigma^{\mathrm{SM}}\left(gg \to H \to \gamma\gamma\right)} = 0.33^{+0.19}_{-0.12} \,. \qquad (1)$$

* Corresponding author.
E-mail addresses: thomas.biekoetter@desy.de (T. Biekötter), Sven.Heinemeyer@cern.ch (S. Heinemeyer), georg.weiglein@desy.de (G. Weiglein).

Here σ^{SM} denotes the cross section for a hypothetical SM Higgs boson at the same mass. In comparison to the previously reported results that were based just on the Run 1 and the first-year Run 2 data [10], the inclusion of the data collected in the second and third year of Run 2 and the refined analysis techniques yield a local significance of the excess that is almost unchanged, while the central value of the signal strength $\mu_{\gamma\gamma}^{\mathrm{exp}}$ in Eq. (1) is substantially smaller than the value $\mu_{\gamma\gamma}^{\mathrm{exp}} = 0.6 \pm 0.2$ extracted from the previous results [10].

Regarding the interpretation of the new result from CMS it is important to note that the updated analysis not only considered more data, but in comparison to Ref. [10] it also improves the background suppression of misidentified $Z \to e^+e^-$ Drell-Yan events, and it includes further event classes requiring the presence of additional jets. Since a possible signal at about 95 GeV giving rise to a relatively small number of events would occur on top of a fluctuating background, one cannot necessarily rely on the naive expectation that the significance of an excess caused by a statistical fluctuation should be reduced by the inclusion of more data while it should be increased in case of an actual signal. In fact, even in the latter case the excess of events observed in the different data sets and evaluated at a fixed mass value would still be expected to fluctuate. From our point of view the fact that the inclusion of the additional data sets and the improvements in the analysis have led to an excess of events at approximately the same mass as previously reported with a statistical significance that has not been reduced strengthens the motivation for exploring a possible BSM origin of the observed results.

ATLAS reported results of searches in the di-photon final state below 125 GeV using 80 fb^{-1} of Run 2 data in 2018 [12]. The ATLAS search found only a mild excess of about 1σ local significance at masses around 95 GeV. However, the cross section limits obtained in the ATLAS analysis are substantially weaker than the corresponding CMS limits, even in the mass range where CMS reported the excess [28], and the excess observed in CMS is therefore compatible with the ATLAS limits.

If the origin of the di-photon excesses at 95 GeV is a new particle, the question arises whether it is also detectable in other collider channels, and whether additional indications for this new particle might have already occurred in other existing searches. Notably, LEP reported a local 2.3σ excess in the $e^+e^- \to Z(H \to b\bar{b})$ searches [6], which would be consistent with a scalar particle with a mass of about 95 GeV.[1] This "$b\bar{b}$ excess" corresponds to a signal strength of $\mu_{bb}^{\mathrm{exp}} = 0.117 \pm 0.057$ [16,29]. Moreover, CMS observed another excess compatible with a mass of 95 GeV in the Higgs-boson searches utilizing di-tau final states [13]. This excess was most pronounced at a mass of 100 GeV with a local significance of 3.1σ, but it is also well compatible with a mass of 95 GeV, where the local significance amounts to 2.6σ. For this "di-tau excess", the best-fit signal strength for a mass hypothesis of 95 GeV was determined to be $\mu_{\tau\tau}^{\mathrm{exp}} = 1.2 \pm 0.5$. It is noteworthy that, to date, ATLAS has not published a search in the di-tau final state that covers the mass range around 95 GeV.

Given that the excesses observed by CMS and LEP occurred at a similar mass, the intriguing question arises whether the excesses in the three different channels might arise from the production of a single new particle. This triggered activities in the literature regarding possible model interpretations that could account for the various excesses while also satisfying all other measurements related to the Higgs sector. Models in which the previously observed two excesses in the di-photon and the $b\bar{b}$ final states can be described simultaneously (with the CMS excess based only on the

Run 1 and first year Run 2 data) were reviewed in Refs. [28,30]. In Ref. [23] those two excesses were studied in the Two-Higgs doublet model (2HDM) with an additional real singlet (N2HDM), with several follow-up analyses [31–33], while in Refs. [34,35] also the more recently observed excess in the di-tau searches was taken into account.

Since the new result obtained by CMS confirmed the previously observed di-photon excess at about 95 GeV but resulted in a significant change in the required signal rate $\mu_{\gamma\gamma}^{\mathrm{exp}}$, it is of interest to assess the implications of the new result on possible model interpretations. In the present paper we focus in particular on the extension of the 2HDM by a complex singlet (S2HDM) as a template for a model where a mostly gauge-singlet scalar particle obtains its couplings to fermions and gauge bosons via the mixing with the SM-like Higgs boson at 125 GeV. We will demonstrate that this kind of scenario is suitable for describing the di-photon excess. In this context we will in particular investigate the impact of the reduced central value of the signal strength of $\mu_{\gamma\gamma}^{\mathrm{exp}} = 0.33$ [15] compared to the result of $\mu_{\gamma\gamma}^{\mathrm{exp}} = 0.6$ that was obtained based on the previous analysis [10]. Moreover, we will discuss the possibility of simultaneously describing the $b\bar{b}$ excess and the di-tau excess. We will further discuss possible ways in which the presented scenario could be confirmed or excluded experimentally in the near future.

The paper is structured as follows. In Sect. 2.1 we introduce the S2HDM and define our notation. In Sect. 2.2 we qualitatively discuss how sizable signal rates in the three channels in which the excesses have been observed can arise. The relevant theoretical and experimental constraints on the model parameters are discussed in Sect. 2.3. We present our numerical results and discuss their implications in Sect. 3, including an analysis of future experimental prospects. The conclusions and an outlook are given in Sect. 4.

2. A 95 GeV Higgs boson in the S2HDM

In this section we briefly summarize the scalar sector of S2HDM and how the excesses at 95 GeV can be accommodated in this model. We also discuss the relevant experimental and theoretical constraints that we apply in our numerical analysis.

2.1. Model definitions

In the SM the Higgs sector contains a single SU(2) doublet Φ_1. The S2HDM extends the SM by a second Higgs doublet field Φ_2 and an additional complex gauge-singlet field Φ_S [31,36]. The richer structure of the scalar sector is motivated for instance by the possibility of a first-order electroweak phase transition [37], and the related phenomenology, including electroweak baryogenesis, or the presence of a stochastic primordial gravitational-wave background. From a more theoretical perspective, the presence of a second Higgs doublet field arises in several extensions of the SM that address the hierarchy problem in the context of supersymmetry [38] or compositeness [39], and in many models addressing the strong CP problem of QCD [40]. Due to the presence of the complex scalar singlet field, the S2HDM can accommodate a dark-matter candidate in the form of pseudo-Nambu-Goldstone (pNG) dark matter [41]. As will be discussed below, among the various proposed WIMP dark-matter candidates, pNG dark matter is in particular motivated in view of the existing limits from dark-matter direct-detection experiments [42–44].

The vacuum state of the S2HDM is characterized by non-zero vacuum expectation values (vev) v_1 and v_2 for the neutral CP-even components of the Higgs doublets fields Φ_1 and Φ_2, respectively. The presence of these vevs leads to the spontaneous breaking of the electroweak symmetry. As in the usual 2HDM, one defines the

---

[1] Due to the $b\bar{b}$ final state the mass resolution is significantly worse compared to the resolution of searches in the di-photon final state.

parameter $\tan\beta = v_2/v_1$, where $v_1^2 + v_2^2 = v^2 \approx (246 \text{ GeV})^2$ corresponds to the SM vev squared. In addition, the real component of the singlet field has the non-zero vev v_S, which breaks a global $U(1)$ symmetry under which only Φ_S is charged. If this symmetry was exact initially, the imaginary component of Φ_S would act as a massless Goldstone boson. Therefore, one introduces a soft breaking via a bilinear term $-m_\chi^2(\Phi_S^2 + \text{h.c.})$, which gives rise to a mass m_χ for the imaginary component of Φ_S, which then plays the role of the pNG dark-matter state.

Neglecting possible sources of CP violation, as we do throughout this paper, the physical scalar spectrum of the S2HDM consists of three CP-even Higgs bosons $h_{1,2,3}$ with masses $m_{h_{1,2,3}}$ that are mixed states composed of the neutral real components of $\Phi_{1,2}$ and the real component of Φ_S. The imaginary component of Φ_S does not mix with other states and results in a stable scalar dark-matter particle which is labelled χ in the following. Moreover, as in the CP-conserving 2HDM, the scalar spectrum contains a pair of charged Higgs bosons $H^\pm$ and a CP-odd Higgs boson A with masses $m_{H^\pm}$ and m_A, respectively.

For the presence of two Higgs doublets, the most general gauge invariant Yukawa sector gives rise to flavour-changing neutral currents (FCNC) at the tree-level. These are, however, strongly constrained experimentally. In order to avoid FCNC at the tree-level, we impose an additional Z_2 symmetry under which one of the doublet fields changes the sign, which is only softly-broken via a term of the form $-m_{12}^2(\Phi_1^\dagger \Phi_2 + \text{h.c.})$. This symmetry can be extended to the fermion sector such that either Φ_1 or Φ_2 (but not both) couples to either the charged leptons ℓ, the up-type quarks u or the down-type quarks d. There are four different possibilities to assign conserved charges for the three kinds of fermions, giving rise to the four Yukawa types I, II, III (lepton-specific) and IV (flipped) that are known from the Z_2-symmetric 2HDM (see e.g. Ref. [45]).

For the Yukawa types II and IV, Φ_1 is coupled to down-type quarks and Φ_2 is coupled to up-type quarks. In this case an independent modification of the couplings of the Higgs bosons h_i to bottom quarks and top quarks is possible. These two types are therefore of particular interest regarding the prediction of a sufficiently large di-photon signal rate [23].

2.2. Interpretation of the excesses

In the following discussion, the lightest of the three CP-even Higgs bosons of the S2HDM h_1 serves as the possible particle state at 95 GeV, also denoted h_{95} from here on. We furthermore assume that the second lightest Higgs boson, $h_2 = h_{125}$, corresponds to the state discovered at about 125 GeV. The key aspect of the signal interpretation presented here is that h_{95} obtains its couplings to the fermions and gauge bosons as a result of the mixing with the CP-even components of the two doublets. In order to comply with the constraints from the Higgs-boson searches at LEP in the mass region of about 95 GeV and the LHC cross section measurements for the detected state at 125 GeV, the state h_{95} must have couplings to gauge-bosons that are reduced by roughly one order of magnitude as compared to the couplings of a SM Higgs boson of the same mass. As a consequence, in the S2HDM interpretation h_{95} is dominantly singlet-like.

Despite the predominant singlet-like character of h_{95}, sizable decay rates into di-photon pairs can be achieved via a suppression of the otherwise dominating decay into b-quark pairs (see also Ref. [46]). At the same time, no such suppression should occur for the coupling to top quarks, whose loop contribution gives rise to the decay into photons (and also governs the production process via gluon fusion). As a result, large signal rates $\mu_{\gamma\gamma}$ can occur in the S2HDM if $|c_{h_{95}t\bar{t}}/c_{h_{95}b\bar{b}}| > 1$, where the coupling coefficients $c_{h_{95}t\bar{t}}$ and $c_{h_{95}b\bar{b}}$ are the couplings of h_{95} to the respective

quark normalized to the couplings of a hypothetical SM Higgs boson of the same mass. It becomes apparent that the Yukawa types I and III, for which $c_{h_{95}t\bar{t}} = c_{h_{95}b\bar{b}}$ applies, do not feature the conditions for a sufficiently large di-photon branching ratio in accordance with the CMS excess. On the other hand, in type II and type IV the two coupling coefficients can be modified independently. This can potentially enhance the di-photon branching ratio by up to an order of magnitude [23,34], such that sizable values of $\mu_{\gamma\gamma}$ can be accommodated even for a relatively small mixing with the detected Higgs boson at 125 GeV (and thus suppressed cross sections).[2]

Since larger values of $\mu_{\gamma\gamma}$ can be achieved in type II and IV compared to type I and type III as discussed above, we will focus on the type II and the type IV in the following. Between these two types, an important difference arises from the fact that $c_{h_{95}\tau^+\tau^-} = c_{h_{95}b\bar{b}}$ holds in type II, whereas the corresponding relation in type IV is $c_{h_{95}\tau^+\tau^-} = c_{h_{95}t\bar{t}}$. Accordingly, in the parameter regions of type II where the di-photon signal rate is enhanced as a consequence of the suppression of its coupling to b-quark pairs the coupling of h_{95} to tau-leptons is simultaneously suppressed. Hence, type II is not expected to yield sizable signal rates in the $\tau^+\tau^-$ decay channel if the di-photon excess is accommodated. On the other hand, given that $c_{h_{95}t\bar{t}}$ should be unsuppressed for a description of the di-photon excess, type IV can give rise to a simultaneous description of the CMS di-tau excess [34].

2.3. Constraints

The parameter space that is relevant for a possible description of the excesses at 95 GeV is subject to various theoretical and experimental constraints. We will briefly discuss the relevant constraints in the following.

Theoretical constraints that we apply in our analysis ensure that the perturbative treatment of the scalar sector of the S2HDM is valid. To this end, we demand that the eigenvalues of the scalar 2×2 scattering matrix in the high-energy limit are smaller than 8π, giving rise to the so-called tree-level perturbative unitarity constraints [31]. In addition, using the approach described in Ref. [31] we apply a condition on the stability of the electroweak vacuum (see Sect. 2.1) by requiring that the tree-level scalar potential is bounded from below, and that the electroweak vacuum corresponds to the global minimum of the potential.

Moreover, the parameters of the S2HDM are constrained by various experimental results. With regards to the collider phenomenology, we check whether the parameter points are in agreement with the cross section limits from collider searches for BSM Higgs bosons by making use of the public code `HiggsBounds v.6` [47–51] (as part of the new code `HiggsTools` [51]). A parameter point is rejected if the signal rate of one of the Higgs bosons in the most sensitive search channel (based on the expected limits) is larger than the experimentally observed limit at the 95% confidence level.

In order to ensure that the properties of h_{125} are in agreement with the measured signal rates from the LHC, we make use of the public code `HiggsSignals v.3` [51–54] (as part of the new code `HiggsTools` [51]). This code performs a χ^2 fit to a large dataset of LHC cross section measurements in the different channels in which the SM-like Higgs boson was observed. As a requirement for accepting or rejecting a parameter point, we use the condition $\chi_{125}^2 \leq \chi_{SM,125}^2 + 6.18$, where χ_{125}^2 is the fit value

---

[2] An additional, although not as significant, enhancement of $\mu_{\gamma\gamma}$ can occur if $c_{h_{95}t\bar{t}}$ and $c_{h_{95}b\bar{b}}$ carry a relative minus sign. This relative sign gives rise to constructive interference effects in the loop-induced couplings of h_{95} to gluons and photons, hence enhancing both the production and the decay rate in the $gg \to h_{95} \to \gamma\gamma$ channel.

of the S2HDM parameter point under consideration, and $\chi^2_{\text{SM,125}} = 146.15$ is the fit result assuming a Higgs boson at 125 GeV that behaves according to the predictions of the SM. In two-dimensional parameter planes the above condition ensures that the selected S2HDM parameter points are not disfavoured by more than 2σ in comparison to the SM regarding the properties of h_{125}.

Both HiggsBounds and HiggsSignals require as input the cross sections and the branching ratios of the scalar state for the considered parameter point. The cross sections were derived internally in HiggsBounds from the effective couplings coefficients. For the computation of the branching ratios, we applied the library N2HDECAY [55,56], which we modified to account for decays of the Higgs bosons into pairs of the DM state χ [31].

Indirect experimental constraints on the Higgs sector can be obtained from flavour-physics observables and from electroweak precision observables. Lacking precise theoretical predictions for the different flavour observables in the S2HDM, we apply conservative lower limits of $\tan\beta > 1.5$ and $m_{H^\pm} > 600$ GeV in our S2HDM parameter scans in type II and type IV to ensure agreement with the flavour-physics constraints [57]. With regards to the electroweak precision observables, we apply constraints in terms of the oblique parameters S, T and U which we computed according to Ref. [58] at the one-loop level. We required that the predicted values of the oblique parameters are in agreement with the fit result of Ref. [57] within a confidence level of 2σ.[3]

As a consequence of the presence of the stable scalar state χ, further constraints on the S2HDM parameter space arise from the measurements of the dark-matter relic abundance of the universe. Assuming the freezout mechanism for the production of χ in the early universe, we applied the Planck measurement of today's relic abundance of $h^2\Omega = 0.119$ [60] as an upper limit, thus avoiding overproduction of dark matter. The theoretical predictions for the relic abundance of χ were obtained by making use of the public code micrOMEGAs [61].

Given its nature as a pNG boson of the softly-broken global U(1) symmetry, the cross sections for the scattering of χ on nuclei are highly suppressed in the limit of small momentum transfer as relevant for dark-matter direct detection experiments [41]. As a result, it has been shown that even including loop corrections the current direct detection constraints are of minor importance in the S2HDM [62]. We nevertheless applied the currently strongest spin-independent cross section limits for the scattering of χ on nucleons obtained by the LZ collaboration [44], where we used the one-loop predictions of the scattering cross sections as computed in Ref. [62].[4]

We finally note that the DM constraints that are imposed in our analysis could also be evaded entirely assuming that the U(1) symmetry acting on Φ_S is gauged [63]. In this case the imaginary component of Φ_S in general is not stable. In an effective field theory framework, the decay is described by higher-dimensional operators that are suppressed by powers of the U(1)-breaking scale. Depending on the size of this scale, the lifetime of χ could be comparable or larger than the age of the universe, in which case χ can still be a viable candidate for (decaying) DM, or χ could be short-lived and thus would not contribute to the DM relic abun-

dance. In the latter case, the constraints from the measured DM relic abundance and DM direct detection experiments do not apply, but on the other hand in this case the model looses the attractive feature of providing a pNG DM state. The most studied model realizations of this kind assume that the U(1) corresponds to a gauged $U(1)_L$ [64] or $U(1)_{B-L}$ [65–67] symmetry, where L and B stand for lepton number and baryon number, respectively, such that Φ_S carries lepton number and can in particular decay into neutrinos. Another possibility is a hidden $U(1)_D$ symmetry in the dark sector, where the kinetic mixing between the $U(1)_D$ and $U(1)_Y$ gauge fields is responsible for the decay of χ [68]. In any case, our conclusions regarding the description of the excesses at 95 GeV do not rely on the application of the DM constraints, see also the discussion below.

3. Numerical discussion

In order to address the question whether a description of the CMS di-photon excess can be realized in the S2HDM, possibly in combination with the excesses in the $b\bar{b}$ and the di-tau final states, we performed a parameter scan in the Yukawa types II and IV of the S2HDM. We investigated the theoretical predictions in comparison to the experimental results for the observed excesses near 95 GeV, ensuring at the same time that the properties of the Higgs boson at 125 GeV are in good agreement with the most up-to-date LHC signal rate measurements. To this end, we implemented a genetic algorithm (using the python package DEAP [69]) that minimizes a loss function constructed from χ^2_{125} (obtained using HiggsSignals) and the three contributions $\chi^2_{\gamma\gamma}$, χ^2_{bb}, and $\chi^2_{\tau\tau}$ quantifying the compatibility with the excesses at 95 GeV, where we define the latter as

$$\chi^2_{\gamma\gamma,\tau\tau,bb} = \frac{(\mu_{\gamma\gamma,\tau\tau,bb} - \mu^{\text{exp}}_{\gamma\gamma,\tau\tau,bb})^2}{(\Delta\mu^{\text{exp}}_{\gamma\gamma,\tau\tau,bb})^2} . \tag{2}$$

Here the experimental central values and the uncertainties were stated in Sect. 1, and $\mu_{\gamma\gamma,\tau\tau,bb}$ are the theoretically predicted values. Since $\mu^{\text{exp}}_{\gamma\gamma}$ has asymmetric uncertainties, we define $\chi^2_{\gamma\gamma}$ in such a way that the lower uncertainty is used if $\mu_{\gamma\gamma} < \mu^{\text{exp}}_{\gamma\gamma}$, and the upper uncertainty is used if $\mu_{\gamma\gamma} > \mu^{\text{exp}}_{\gamma\gamma}$. To obtain the predictions for $\mu_{\gamma\gamma}$ and $\mu_{\tau\tau}$, we used HiggsTools to derive the gluon-fusion cross section of the state at 95 GeV via a re-scaling of the SM predictions as a function of $c_{h_{95}t\bar{t}}$ and $c_{h_{95}b\bar{b}}$. To compute μ_{bb}, we approximated the cross section ratio as $\sigma/\sigma_{\text{SM}} = c^2_{h_{95}VV}$. The branching ratios of h_{95} were obtained with the help of N2HDECAY (see also the discussion in Sect. 2.3).

The set of parameter points obtained by the minimization of the loss function was then confronted with the constraints discussed in Sect. 2.3. Parameter points that did not pass the applied constraints were rejected. For the generation of the S2HDM parameter points and the application of the constraints, we used the program s2hdmTools [31,62], which features interfaces to HiggsBounds, HiggsSignals, micrOMEGAs and N2HDECAY.

We chose the values of the free parameters in our scan as follows. The mass of h_{95} was varied in the region in which the di-photon excess is most pronounced, i.e. $94\,\text{GeV} \leq m_{h_{95}} \leq 97\,\text{GeV}$. The mass of the second-lightest Higgs boson was set to $m_{h_{125}} = 125.09$ GeV, and the third heavier Higgs boson, denoted H in the following, was scanned freely up to an upper limit of $m_H = 1$ TeV. The same upper limit was chosen for the masses of the DM state χ, the CP-odd Higgs boson A, and the charged Higgs bosons $H^\pm$, where for the latter additionally the lower limit $m_{H^\pm} > 600$ GeV was applied arising from the flavour constraints. Moreover, we varied $\tan\beta$ in the range $1.5 \leq \tan\beta \leq 10$, and for the singlet vev we

---

[3] The fit result of the oblique parameters was obtained before the recent CDF measurement of M_W [59], which showed a significant upward deviation with respect to the SM prediction. We demonstrated in Ref. [35] that a larger value for the W-boson mass, even as large as the central value of the CDF measurement, can be accommodated in a 2HDM that is extended by a singlet if there are sizable mass splittings between the heavy BSM Higgs bosons h_3, A and $H^\pm$, while in addition the excesses at 95 GeV can be accommodated in the same way as presented here.

[4] Dark-matter indirect detection experiments can so far only probe a very limited mass window of m_χ once the experimental upper limit on the relic abundance is applied [31]. Thus, we do not consider additional constraints from indirect-detection experiments.
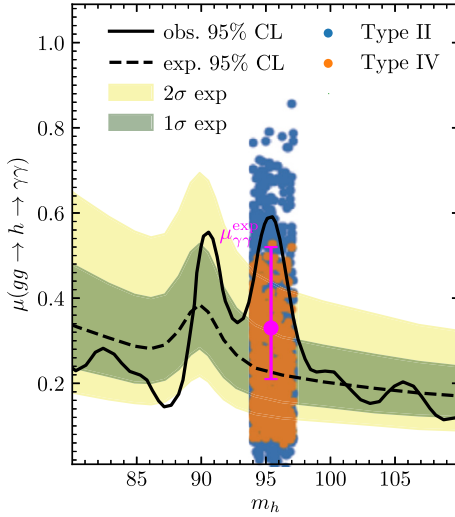
Fig. 1. S2HDM parameter points passing the applied constraints in the $(m_{h_{95}}, \mu_{\gamma\gamma})$ plane for the type II (blue) and the type IV (orange). The expected and observed cross section limits obtained by CMS are indicated by the black dashed and solid lines, respectively, and the 1σ and 2σ uncertainty intervals are indicated by the green and yellow bands, respectively. The value of $\mu_{\gamma\gamma}^{\exp}$ and its uncertainty is shown with the magenta error bar at the mass value at which the excess is most pronounced.

chose $40\text{ GeV} \leq v_S \leq 2\text{ TeV}$. Finally, the scan range of the parameter m_{12}^2 was determined by the condition $400\text{ GeV} \leq M \leq 1\text{ TeV}$, where $M^2 = m_{12}^2/(\sin\beta\cos\beta)$.

3.1. Description of the di-photon excess

In Fig. 1 we show the predictions for $\mu_{\gamma\gamma}$ for the S2HDM parameter points that are in agreement with the applied constraints. The type II parameter points are shown in blue, and the parameter points of type IV are shown in orange. The expected and observed cross section limits obtained by CMS are indicated by the black dashed and solid lines, respectively, and the 1σ and 2σ uncertainty intervals are indicated by the green and yellow bands, respectively [15]. The value of $\mu_{\gamma\gamma}^{\exp}$ and its uncertainty is shown with the magenta error bar at the mass value at which the excess is most pronounced. One can see that both types of the S2HDM considered here can accommodate the observed excess. As expected from the discussion in Sect. 2.2, type II can give rise to larger predicted values of $\mu_{\gamma\gamma}$ due to the additional suppression of the $h_{95} \to \tau^+\tau^-$ decay mode. The points featuring the largest values of $\mu_{\gamma\gamma}$ in type II are seen to exceed the observed limit of the new CMS analysis (which is not applied as a constraint via `HiggsBounds` in this plot). On the other hand, both type II and type IV give rise to predictions for $\mu_{\gamma\gamma}$ that are very well compatible with the new experimental value of $\mu_{\gamma\gamma}^{\exp}$ obtained by CMS after the inclusion of the second- and third-year Run 2 data.[5]

3.2. Combined description of the excesses

We demonstrated in the previous section that both the Yukawa types II and IV can describe the excess in the di-photon channel observed by CMS. Now we turn to the question whether additionally also the $b\bar{b}$ excess observed at LEP and the $\tau^+\tau^-$ excess at CMS can be accommodated.

Starting with the $b\bar{b}$ excess, we show in the top row of Fig. 2 the parameter points passing the applied constraints in the $(\mu_{\gamma\gamma}, \mu_{bb})$ plane. The parameter points of type II and type IV are shown in left and the right plot, respectively. The colours of the points indicate the value of $\Delta\chi_{125}^2$ showing the compatibility with the LHC rate measurements of h_{125}. The black dashed lines indicate the region in which the excesses are described at a level of 1σ or better, i.e. $\chi_{\gamma\gamma}^2 + \chi_{bb}^2 \leq 2.3$ (see Eq. (2)). The shape of these lines is asymmetrical due to the asymmetrical uncertainties of $\mu_{\gamma\gamma}^{\exp}$ used in the definition of $\chi_{\gamma\gamma}^2$ in Eq. (2).

One can see that we find points inside the 1σ preferred region in the upper left and right plots. Thus, both type II and type IV are able to describe the di-photon excess and the $b\bar{b}$ excess simultaneously. At the same time the properties of the second-lightest scalar h_{125} are such that the LHC rate measurements can be accommodated at the same χ^2 level as in the SM, i.e. $\Delta\chi_{125}^2 \approx 0$, or even marginally better, i.e. $\Delta\chi_{125}^2 < 0$. At the current level of experimental precision, the description of both excesses is therefore possible in combination with the presence of a Higgs boson at 125 GeV that would so far be indistinguishable from a SM Higgs boson.

Turning to the di-tau excess, we show in the bottom row of Fig. 2 the parameter points passing the applied constraints in the $(\mu_{\gamma\gamma}, \mu_{\tau\tau})$ plane. As before, the colours of the points indicate the values of $\Delta\chi_{125}^2$, and the black dashed lines indicate the region in which the di-photon excess and the di-tau excess are described at a level of 1σ or better, i.e. $\chi_{\gamma\gamma}^2 + \chi_{\tau\tau}^2 \leq 2.3$.

In the lower left plot, showing the parameter points of the scan in type II, one can see that there are no points within or close to the black line. This finding is in agreement with the discussion in Sect. 2.2. It is also qualitatively unchanged as compared to the results of Ref. [34], where $\mu_{\gamma\gamma}^{\exp} = 0.6 \pm 0.2$ was used: the new and somewhat lower experimental central value of $\mu_{\gamma\gamma}^{\exp}$ has no impact on the (non-)compatibility of the $\gamma\gamma$ and the $\tau^+\tau^-$ excesses in Yukawa type II.

The lower right plot shows the parameter points passing the applied constraints from the scan in type IV. One can observe that the values of $\mu_{\tau\tau}$ overall increase with increasing value of $\mu_{\gamma\gamma}$. The parameter points that predict the largest values for the signal rates reach the lower edge of the black line that indicates the preferred region regarding the two excesses. However, even these points lie substantially below the central value of $\mu_{\tau\tau}^{\exp}$. A simultaneous description of both excesses at 95 GeV observed by CMS is therefore possible only at the level of 1σ at best. Although larger values of $\mu_{\tau\tau}$ are theoretically possible in type IV [34], the application of cross-section limits from Higgs-boson searches exclude such parameter points. These constraints arise in particular from recent searches performed by CMS for the production of a Higgs boson in association with a top-quark pair or in association with a Z boson, with subsequent decay into tau pairs [70].

Constraints on the interpretation of the di-tau excess as an additional Higgs boson were also derived from cross-section measurements of the Higgs boson at 125 GeV. In particular, Ref. [71] investigated the sensitivity of the ATLAS measurement assuming the production of h_{125} in association with a top-quark pair and subsequent decay into di-tau pairs [72].[6] The ATLAS analysis considered an invariant di-tau mass in the range between 50 GeV and 200 GeV and is based on the full Run 2 data set. We emphasize,

---

[5] As discussed above, in type I and type III no significant enhancement of the di-photon branching ratio of h_{95} is possible, and one finds $\mu_{\gamma\gamma} \approx \mu_{bb} \lesssim c_{h_{95}VV}^2$. Thus, $\mu_{\gamma\gamma}$-values close to $\mu_{\gamma\gamma}^{\exp}$ require values of $c_{h_{125}VV}^2 \approx 1 - c_{h_{95}VV}^2$ that are in significant tension with the coupling measurements of h_{125}.

[6] In Ref. [73] the invariant-mass spectra of the $h_{125} \to WW^*$ decay channel measured by ATLAS [74] and CMS [75] were considered. However, the decay of $h_{95} \to WW^*$ is highly off-shell, suppressing the corresponding branching ratio by orders of magnitude compared to the one of h_{125}. As a result, there is no sensitivity in this decay channel to the presence of h_{95} according to our model interpretation of the excesses.
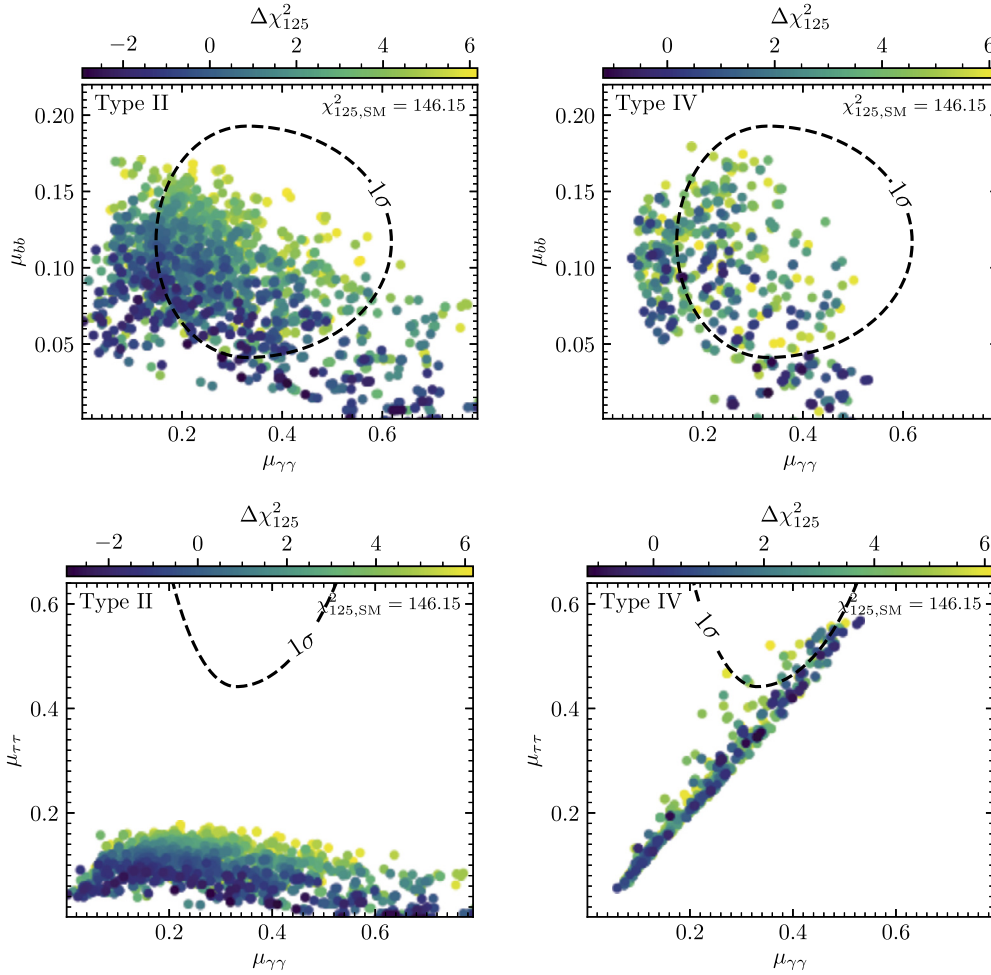
Fig. 2. S2HDM parameter points passing the applied constraints in the $(\mu_{\gamma\gamma}, \mu_{bb})$ plane (top row) and the $(\mu_{\gamma\gamma}, \mu_{\tau\tau})$ plane (bottom row) for type II (left) and type IV (right). The colours of the points indicate the value of $\Delta\chi^2_{125}$. The black dashed lines indicate the regions in which the two excesses considered in each plot are accommodated at a level of 1σ or better, i.e. $\chi^2_{\gamma\gamma} + \chi^2_{bb} \leq 2.3$ (top row) and $\chi^2_{\gamma\gamma} + \chi^2_{\tau\tau} \leq 2.3$ (bottom row).

however, that the constraints extracted in Ref. [71] are affected by the lack of publicly available information on the correlations between the different mass bins.

In summary, the S2HDM type II can simultaneously describe the CMS di-photon excess and the $b\bar{b}$ excess observed at LEP, whereas no significant contribution to the signal strength of the CMS di-tau excess is generated. In type IV, in addition also a contribution to the di-tau signal strength can occur, although the largest possible signal rates of about $\mu_{\tau\tau} = 0.5$ are somewhat below the experimentally preferred range of $\mu_{\tau\tau}^{exp} = 1.2 \pm 0.5$.

Our results in the S2HDM can be generalised to other extended Higgs sectors containing at least a second Higgs doublet and at least one scalar singlet. Our analysis indicates that the conclusions in various models that have previously been considered as an explanation for the di-photon excess are expected to be affected by the modified value of $\mu_{\gamma\gamma}^{exp}$. This applies in particular to supersymmetric extensions of the SM, which were shown to be able to accommodate a signal at about 95 GeV with a signal strength that in most cases was predicted to be at the lower end of the previous $\mu_{\gamma\gamma}^{exp}$-range [20,22,25,32,76–78]. Requiring also agreement with the LEP excess resulted in $\mu_{\gamma\gamma} \approx 0.3$ [22,32,77], which turns out to be in very good agreement with the updated result from CMS.

3.3. Prospects at future colliders

We finally discuss how future collider experiments will shed light on the possible presence of a Higgs boson below 125 GeV as considered here. In the S2HDM the mixing between the singlet-like state at 95 GeV and the SM-like state at 125 GeV determines the strengths of the couplings of h_{95} to fermions and gauge bosons. Thus, in addition to directly searching for h_{95}, a complementary – although more model-dependent – strategy consists in the search for modifications of the cross sections of h_{125} compared to the ones of a SM Higgs boson. We start with discussing this approach in the following.

Currently, the experimental precision of the observed couplings of h_{125} is at the level of ten to twenty percent [3,4]. During the high-luminosity phase of the LHC (HL-LHC), the experimental precision of these couplings is expected to be reduced to the level of a few percent [79].[7] A future e^+e^- collider with sufficient energy to produce h_{125} could further improve the experimental precision to the sub-percent level. As an example, we will consider in the following the expected precision of the International Linear Collider (ILC) operating at a centre-of-mass energy of 250 GeV and collecting 2 ab^{-1} of integrated luminosity [80]. We note that here and in the following the specific example of the projections for the ILC is meant to showcase the potential impact of the coupling measurements at a future e^+e^- collider. In fact, very similar results would be obtained considering the other proposals for a "Higgs factory" operating at about 250 GeV, such as CLIC, CEPC or the FCC-ee [81].

---

[7] Here it is assumed that no undetected decay mode of h_{125} into BSM particles is present.
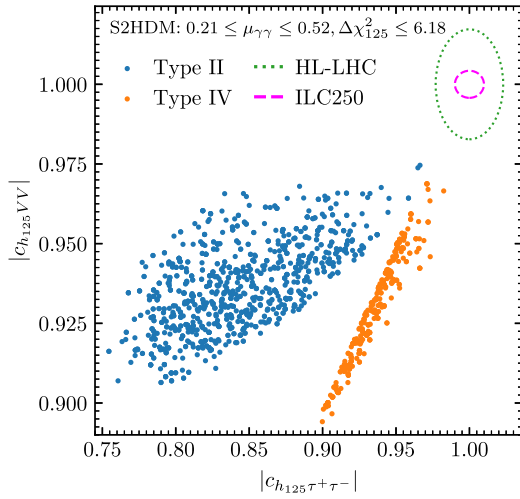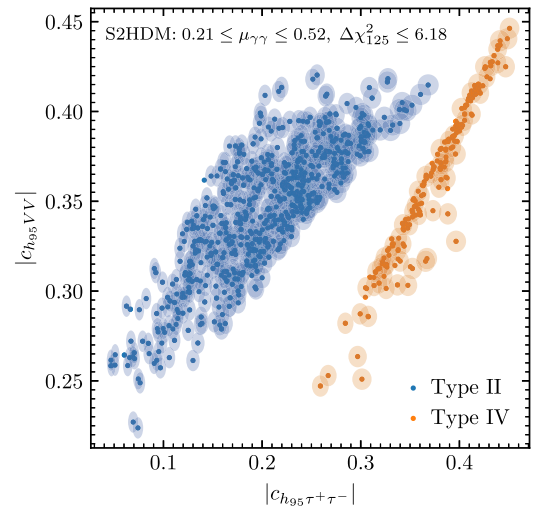
Fig. 3. S2HDM parameter points passing the applied constraints that predict a di-photon signal strength in the preferred range of $0.21 \leq \mu_{\gamma\gamma} \leq 0.52$ in view of the excess observed by CMS [15] in the $(|c_{h_{125}\tau^+\tau^-}|, |c_{h_{125}VV}|)$ plane. The type II and the type IV parameter points are shown in blue and orange, respectively. The green dotted and the magenta dashed ellipses indicate the projected experimental precision of the coupling measurements at the HL-LHC [79] and the ILC250 [80], respectively, with their centres located at the SM values.

Fig. 4. S2HDM parameter points passing the applied constraints that predict a di-photon signal strength in the preferred range $0.21 \leq \mu_{\gamma\gamma} \leq 0.52$ in view of the excess observed by CMS [15] in the $(|c_{h_{95}\tau^+\tau^-}|, |c_{h_{95}VV}|)$ plane. The type II and the type IV parameter points are shown in blue and orange, respectively. The shaded ellipses around the dots indicate the projected experimental precision with which the couplings of h_{95} could be measured at the ILC250 with 2 ab^{-1} of integrated luminosity, which we evaluated according to Ref. [33].

In Fig. 3 we show the parameter points passing the applied constraints of the scan in type II (blue) and in type IV (orange) that provide a good description of the di-photon excess, i.e. $0.21 \leq \mu_{\gamma\gamma} \leq 0.52$, in the $(|c_{h_{125}\tau^+\tau^-}|, |c_{h_{125}VV}|)$ plane. Here $c_{h_{125}\tau^+\tau^-}$ and $c_{h_{125}VV}$ are the effective coefficients of the coupling of h_{125} to tau-leptons and the gauge bosons $V = Z, W$, respectively. These coefficients are normalized such that they are equal to one in the SM. Centred at the SM prediction, we also indicate with the green dotted ellipse the expected precision on the coupling coefficients after the HL-LHC will have collected 3000 fb^{-1} of integrated luminosity. Finally, the magenta dashed ellipse indicates the expected experimental precision after a combination of the HL-LHC data and the ILC data collected at $\sqrt{s} = 250$ GeV (ILC250) with an integrated luminosity of 2 ab^{-1}. We note that these experimental projections have been obtained assuming that the cross section measurements are according to the predictions of the SM.

One can see that the points of both types all lie outside of the green ellipse. For the points with the largest deviations from the SM, the anticipated HL-LHC precision would be sufficient to distinguish between SM-like properties of h_{125} and the predictions of the S2HDM for parameter regions that are in accordance with the observed di-photon excess. However, for the S2HDM points that are closest to the SM value, no distinction at the 2σ level could be established. Consequently, the HL-LHC will not be able to entirely probe the S2HDM interpretation of the di-photon excess at 95 GeV based on the coupling measurements of h_{125}. Moreover, for many of the displayed blue and orange points the expected HL-LHC precision, indicated by the size of the green ellipse, will not be sufficient to distinguish between a type II and a type IV interpretation.

Now we compare the model predictions with the expected precision at the ILC250, indicated by the magenta ellipse. One can see that under the assumption that no modifications of the properties of h_{125} will be observed even at the ILC, all parameter points would be excluded with high experimental significance. On the other hand, for each point in the S2HDM describing the di-photon excess, a clear deviation of the properties of h_{125} from the SM predictions could be established via the coupling measurements. The ILC also has a significantly larger potential to distinguish between a type II and a type IV scenario, although even the ILC precision might not be sufficient to distinguish between the types for the

parameter points with the largest values of $c_{h_{125}\tau^+\tau^-}$ and $c_{h_{125}VV}$. Information about the direct production of h_{95} and its coupling measurements will of course be instrumental to further probe the S2HDM scenarios.

In our S2HDM interpretation of the di-photon excess, h_{95} is required to have a non-vanishing coupling to top quarks, and thus also to gauge bosons, in order to be the origin of this excess. Moreover, a sizable coupling of h_{95} to the Z boson is required if this state is also supposed to be the origin of the $b\bar{b}$ excess observed at LEP. In this case, a future lepton collider running at 250 GeV has the capability to produce h_{95} in large numbers [82,83]. From the resulting cross-section measurements, the couplings of h_{95} could be determined with a precision that is expected to greatly improve on the precision achievable at the LHC.[8] Thus, if a new state at 95 GeV exists, a future e^+e^- collider such as the ILC is expected to be of vital importance for the determination of the underlying model that is realized in nature.

In order to showcase the potential of the ILC for discriminating different models that give rise to the state at h_{95}, we show in Fig. 4 the parameter points of our scans in the $(|c_{h_{95}\tau^+\tau^-}|, |c_{h_{95}VV}|)$ plane. Here, $c_{h_{95}\tau^+\tau^-}$ and $c_{h_{95}VV}$ are the effective coefficients for the couplings of h_{95} to tau-leptons and gauge bosons, respectively. These coefficients are normalized such that they are equal to one for a hypothetical SM Higgs boson at the mass of h_{95}. As in Fig. 3, the parameter points of type II and type IV are shown in blue and orange, respectively, and we only depict the parameter points that provide a good description of the di-photon excess observed by CMS. In addition to the theoretical prediction of the coupling

---

[8] Experimental projections for Higgs coupling measurements at the HL-LHC are only publicly available for the discovered Higgs boson at 125 GeV. In contrast to the cleaner experimental environment at an e^+e^- collider, at the LHC it is not feasible to obtain projections for the accuracy of coupling measurements for additional Higgs bosons without detailed simulations taking into account systematical uncertainties. Since such a dedicated simulation would be beyond the scope of the present paper, we do not attempt to provide precise quantitative estimates for the achievable accuracy on the couplings of h_{95} at the HL-LHC. However, a rough estimate of the precision for the signal rates in the di-photon and di-tau channel assuming 3 ab^{-1} can be achieved by a simple rescaling with the square root of the luminosity, yielding a precision of about 10% for the di-photon and the di-tau channel.

coefficients, indicated with the dots, we also indicated the experimental precision with which the respective couplings could be measured at the ILC by means of the shaded ellipses around each dot. We estimated the experimental precision of the coupling measurements for the ILC250 with 2 ab^{-1} of integrated luminosity according to the approach discussed in Ref. [33].

One can observe in Fig. 4 that the blue points and the orange points are clearly separated from each other. For a fixed value of the gauge-boson coupling, the parameter points of type IV predict larger couplings to tau-leptons compared to the parameter points of type II. This is in line with the discussion in Sect. 2.2: In type II one has $c_{h_{95}\tau^+\tau^-} = c_{h_{95}b\bar{b}}$, such that the enhancement of the di-photon branching ratio via the condition $|c_{h_{95}t\bar{t}}/c_{h_{95}b\bar{b}}| > 1$ is achieved in the regime in which $c_{h_{95}\tau^+\tau^-}$ is suppressed. On the other hand, in type IV one has $c_{h_{95}\tau^+\tau^-} = c_{h_{95}t\bar{t}}$, such that the coupling to tau-leptons is less suppressed in the regime in which the di-photon branching ratio is enhanced.

As a consequence of the separation of the points of the two types, combined with the high anticipated precision of the h_{95} coupling measurements at the ILC250, there are no blue or orange ellipses that overlap. Thus, the coupling measurements of h_{95} at the ILC would be sufficient to distinguish between a type II or a type IV interpretation. In combination with the experimental observation regarding h_{125} (see discussion above), a lepton collider like the ILC would be able to scrutinize the underlying physics model that is realized in nature.

4. Conclusions and outlook

Recently, upon the inclusion of the full Run 2 data set and substantially refined analysis techniques, the CMS collaboration has confirmed an excess of about 3σ local significance at about 95 GeV in the low-mass Higgs boson searches in the di-photon final state. An excess at this mass value with similar significance had previously been reported based on the 8 TeV Run 1 and the first-year Run 2 data set. We have investigated the interpretation of this excess as a di-photon resonance arising from the production of a Higgs boson in the Two-Higgs doublet model that is extended by a complex singlet (S2HDM). We have shown that a good description of the excess is possible in the Yukawa type II and IV, while being in agreement with all other collider searches for additional Higgs bosons, the measurements of the properties of the SM-like Higgs boson at 125 GeV, and further experimental and theoretical constraints. At the same time, the model can account for all or a large fraction of the observed DM relic abundance in agreement with the measurements of the Planck satellite.

Previously, a signal strength for the di-photon excess observed by CMS of $\mu_{\gamma\gamma}^{\mathrm{exp}} = 0.6 \pm 0.2$ had been obtained utilizing the data from the first year of Run 2 and of Run 1. This relatively high central value of the signal strength gave rise to a preference to a type II Yukawa structure, in which larger signal rates of the state at 95 GeV can be achieved compared to the type IV. After the inclusion of the remaining Run 2 data and performing various improvements of the experimental analysis, the new CMS result shows an excess with a local significance that is essentially unchanged compared to the previous result but which yields an interpretation in terms of a smaller central value of the signal strength with reduced uncertainties, $\mu_{\gamma\gamma}^{\mathrm{exp}} = 0.33^{+0.19}_{-0.12}$. We have shown that as a result of the smaller central value of $\mu_{\gamma\gamma}^{\mathrm{exp}}$ both Yukawa types provide an equally well description of the di-photon excess in the S2HDM.

The di-photon excess observed at CMS is especially intriguing in view of additional excesses that appeared at approximately the same mass. An excess of events above the SM expectation with about 2σ local significance was observed at LEP in searches for Higgsstrahlung production of a scalar state that then decays to a pair of bottom quarks. Moreover, CMS observed an excess

with about 3σ local significance consistent with a mass of about 95 GeV in searches for the production of a Higgs boson via gluon fusion and subsequent decay into tau pairs.

We have demonstrated that the S2HDM type II can simultaneously describe the CMS di-photon excess and the $b\bar{b}$ excess observed at LEP, whereas no significant signal for the CMS di-tau excess is possible in this model. In the S2HDM type IV, on the other hand, in addition also a sizable signal strength in the di-tau channel can occur. However, even in type IV the maximally reachable signal rates are smaller than the signal strengths that would be required to describe the di-tau excess at the level of 1σ.

Our analysis in the S2HDM serves as an example study from which more general conclusions valid for a wider class of extensions of the SM can be drawn. Notably, supersymmetric extensions were previously shown to be able to accommodate a di-photon signal at about 95 GeV that turns out to be in good agreement with the updated experimental value of $\mu_{\gamma\gamma}^{\mathrm{exp}}$.

In the near future, the possible presence of a Higgs boson at 95 GeV can be directly tested by the eagerly awaited results from the corresponding ATLAS searches in the di-photon and the di-tau final states covering the mass region below 125 GeV and utilizing the full Run 2 data. Further into the future, the scenarios discussed here will be tested in a twofold way at future Runs of the (HL-)LHC, where the direct searches for h_{95} and the coupling measurements of h_{125} will benefit in particular from a significant increase of statistics. Nevertheless, we have shown that the experimental precision of the coupling measurements of the Higgs boson at 125 GeV might not be sufficient to exclude the S2HDM interpretation of the excesses at 95 GeV, or conversely confirm a deviation from the SM predictions.

Going beyond the (HL-)LHC projections, we have discussed the experimental prospects at a future e^+e^- collider, considering as an example the ILC operating at 250 GeV with an integrated luminosity of 2 ab^{-1}. At the ILC250, the couplings of h_{125} could be determined in an effectively model independent way at subpercent level precision. Assuming that no deviations from the SM predictions would be observed, the measurements of the couplings of h_{125} would significantly disfavour the S2HDM interpretation of the excess at 95 GeV. Conversely, a clear deviation from the SM predictions will be established if the coupling measurements of h_{125} will be according to the predictions of any S2HDM parameter point describing the excess.

Although the possible state at 95 GeV has suppressed couplings compared to h_{125}, the ILC could produce h_{95} in large numbers if it has a sufficiently large coupling to Z bosons. We have shown that the clean environment of an e^+e^- collider would allow for a determination of the couplings of h_{95} at percent-level precision. As such, we demonstrated that the ILC, in contrast to the HL-LHC, could distinguish between a type II and a type IV description of the excesses.

Declaration of competing interest

The authors declare that they have no known competing financial interests or personal relationships that could have appeared to influence the work reported in this paper.

Data availability

Data will be made available on request.

Acknowledgements

References

[1] ATLAS collaboration, Observation of a new particle in the search for the standard model Higgs boson with the ATLAS detector at the LHC, Phys. Lett. B 716 (2012) 1, arXiv:1207.7214.

[2] CMS collaboration, Observation of a new boson at a mass of 125 GeV with the CMS experiment at the LHC, Phys. Lett. B 716 (2012) 30, arXiv:1207.7235.

[3] CMS collaboration, A portrait of the Higgs boson by the CMS experiment ten years after the discovery, Nature 607 (2022) 60, arXiv:2207.00043.

[4] ATLAS collaboration, A detailed map of Higgs boson interactions by the ATLAS experiment ten years after the discovery, Nature 607 (2022) 52, arXiv:2207.00092.

[5] OPAL collaboration, Decay mode independent searches for new scalar bosons with the OPAL detector at LEP, Eur. Phys. J. C 27 (2003) 311, arXiv:hep-ex/0206022.

[6] LEP Working Group for Higgs Boson searches, ALEPH, DELPHI, L3, OPAL collaboration, Search for the standard model Higgs boson at LEP, Phys. Lett. B 565 (2003) 61, arXiv:hep-ex/0306033.

[7] LEP Working Group for Higgs Boson Searches, ALEPH, DELPHI, L3, OPAL collaboration, Search for neutral MSSM Higgs bosons at LEP, Eur. Phys. J. C 47 (2006) 547, arXiv:hep-ex/0602042.

[8] CDF, D0 collaboration, Updated combination of CDF and D0 searches for standard model Higgs boson production with up to 10. 0 fb^{-1} of data, July 2012, arXiv:1207.0449.

[9] CMS collaboration, Search for new resonances in the diphoton final state in the mass range between 80 and 110 GeV in pp collisions at $\sqrt{s} = 8$ TeV, Tech. Rep. CMS-PAS-HIG-14-037, 2015.

[10] CMS collaboration, Search for a standard model-like Higgs boson in the mass range between 70 and 110 GeV in the diphoton final state in proton-proton collisions at $\sqrt{s} = 8$ and 13 TeV, Phys. Lett. B 793 (2019) 320, arXiv:1811.08459.

[11] CMS collaboration, Search for additional neutral MSSM Higgs bosons in the $\tau\tau$ final state in proton-proton collisions at $\sqrt{s} = 13$ TeV, J. High Energy Phys. 09 (2018) 007, arXiv:1803.06553.

[12] ATLAS collaboration, Search for resonances in the 65 to 110 GeV diphoton invariant mass range using 80 fb^{-1} of pp collisions collected at $\sqrt{s} = 13$ TeV with the ATLAS detector, Tech. Rep. ATLAS-CONF-2018-025, 2018.

[13] CMS collaboration, Searches for additional Higgs bosons and for vector leptoquarks in $\tau\tau$ final states in proton-proton collisions at $\sqrt{s} = 13$ TeV, arXiv:2208.02717.

[14] ATLAS collaboration, Search for boosted diphoton resonances in the 10 to 70 GeV mass range using 138 fb^{-1} of 13 TeV pp collisions with the ATLAS detector, arXiv:2211.04172.

[15] CMS collaboration, Search for low mass resonances in the diphoton final state in proton-proton collisions at $\sqrt{s} = 13$ TeV with the full Run 2 dataset, Tech. Rep. CMS-HIG-20-002, 2023.

[16] J. Cao, X. Guo, Y. He, P. Wu, Y. Zhang, Diphoton signal of the light Higgs boson in natural NMSSM, Phys. Rev. D 95 (2017) 116001, arXiv:1612.08522.

[17] P.J. Fox, N. Weiner, Light signals from a lighter Higgs, J. High Energy Phys. 08 (2018) 025, arXiv:1710.07649.

[18] F. Richard, Search for a light radion at HL-LHC and ILC250, arXiv:1712.06410.

[19] U. Haisch, A. Malinauskas, Let there be light from a second light Higgs doublet, J. High Energy Phys. 03 (2018) 135, arXiv:1712.06599.

[20] T. Biekötter, S. Heinemeyer, C. Muñoz, Precise prediction for the Higgs-boson masses in the $\mu\nu$ SSM, Eur. Phys. J. C 78 (2018) 504, arXiv:1712.07475.

[21] D. Liu, J. Liu, C.E.M. Wagner, X.-P. Wang, A light Higgs at the LHC and the B-anomalies, J. High Energy Phys. 06 (2018) 150, arXiv:1805.01476.

[22] F. Domingo, S. Heinemeyer, S. Paßehr, G. Weiglein, Decays of the neutral Higgs bosons into SM fermions and gauge bosons in the $\mathcal{CP}$-violating NMSSM, Eur. Phys. J. C 78 (2018) 942, arXiv:1807.06322.

[23] T. Biekötter, M. Chakraborti, S. Heinemeyer, A 96 GeV Higgs boson in the N2HDM, Eur. Phys. J. C 80 (2020) 2, arXiv:1903.11661.

[24] J.M. Cline, T. Toma, Pseudo-Goldstone dark matter confronts cosmic ray and collider anomalies, Phys. Rev. D 100 (2019) 035023, arXiv:1906.02175.

[25] J. Cao, X. Jia, Y. Yue, H. Zhou, P. Zhu, 96 GeV diphoton excess in seesaw extensions of the natural NMSSM, Phys. Rev. D 101 (2020) 055008, arXiv:1908.07206.

[26] J.A. Aguilar-Saavedra, F.R. Joaquim, Multiphoton signals of a (96 GeV?) stealth boson, Eur. Phys. J. C 80 (2020) 403, arXiv:2002.07697.

[27] S. Gascon-Shotkin, CMS, Talk at MoriondEW: searches for additional Higgs bosons at low mass, indico.cern.ch, 2023.

[28] S. Heinemeyer, T. Stefaniak, A Higgs boson at 96 GeV?!, PoS CHARGED2018 (2019) 016, arXiv:1812.05864.

[29] A. Azatov, R. Contino, J. Galloway, Model-independent bounds on a light Higgs, J. High Energy Phys. 04 (2012) 127, arXiv:1202.3415.

[30] S. Heinemeyer, A Higgs boson below 125 GeV?!, Int. J. Mod. Phys. A 33 (2018) 1844006.

[31] T. Biekötter, M.O. Olea-Romacho, Reconciling Higgs physics and pseudo-Nambu-Goldstone dark matter in the S2HDM using a genetic algorithm, J. High Energy Phys. 10 (2021) 215, arXiv:2108.10864.

[32] T. Biekötter, A. Grohsjean, S. Heinemeyer, C. Schwanenberger, G. Weiglein, Possible indications for new Higgs bosons in the reach of the LHC: N2HDM and NMSSM interpretations, Eur. Phys. J. C 82 (2022) 178, arXiv:2109.01128.

[33] S. Heinemeyer, C. Li, F. Lika, G. Moortgat-Pick, S. Paasch, Phenomenology of a 96 GeV Higgs boson in the 2HDM with an additional singlet, Phys. Rev. D 106 (2022) 075003, arXiv:2112.11958.

[34] T. Biekötter, S. Heinemeyer, G. Weiglein, Mounting evidence for a 95 GeV Higgs boson, J. High Energy Phys. 08 (2022) 201, arXiv:2203.13180.

[35] T. Biekötter, S. Heinemeyer, G. Weiglein, Excesses in the low-mass Higgs-boson search and the W-boson mass measurement, arXiv:2204.05975.

[36] X.-M. Jiang, C. Cai, Z.-H. Yu, Y.-P. Zeng, H.-H. Zhang, Pseudo-Nambu-Goldstone dark matter and two-Higgs-doublet models, Phys. Rev. D 100 (2019) 075011, arXiv:1907.09684.

[37] T. Biekötter, S. Heinemeyer, J.M. No, M.O. Olea, G. Weiglein, Fate of electroweak symmetry in the early universe: non-restoration and trapped vacua in the N2HDM, J. Cosmol. Astropart. Phys. 06 (2021) 018, arXiv:2103.12707.

[38] P. Fayet, Supersymmetry and weak, electromagnetic and strong interactions, Phys. Lett. B 64 (1976) 159.

[39] J. Mrazek, A. Pomarol, R. Rattazzi, M. Redi, J. Serra, A. Wulzer, The other natural two Higgs doublet model, Nucl. Phys. B 853 (2011) 1, arXiv:1105.5403.

[40] J.E. Kim, Light pseudoscalars, particle physics and cosmology, Phys. Rep. 150 (1987) 1.

[41] V. Barger, P. Langacker, M. McCaskey, M. Ramsey-Musolf, G. Shaughnessy, Complex singlet extension of the standard model, Phys. Rev. D 79 (2009) 015018, arXiv:0811.0393.

[42] PandaX-4T collaboration, Dark matter search results from the PandaX-4T commissioning run, Phys. Rev. Lett. 127 (2021) 261802, arXiv:2107.13438.

[43] XENON collaboration, Dark matter search results from a one ton-year exposure of XENON1T, Phys. Rev. Lett. 121 (2018) 111302, arXiv:1805.12562.

[44] LZ collaboration, First dark matter search results from the LUX-ZEPLIN (LZ) experiment, arXiv:2207.03764.

[45] G.C. Branco, P.M. Ferreira, L. Lavoura, M.N. Rebelo, M. Sher, J.P. Silva, Theory and phenomenology of two-Higgs-doublet models, Phys. Rep. 516 (2012) 1, arXiv:1106.0034.

[46] R. Barbieri, D. Buttazzo, K. Kannike, F. Sala, A. Tesi, One or more Higgs bosons?, Phys. Rev. D 88 (2013) 055011, arXiv:1307.4937.

[47] P. Bechtle, O. Brein, S. Heinemeyer, G. Weiglein, K.E. Williams, HiggsBounds: confronting arbitrary Higgs sectors with exclusion bounds from LEP and the tevatron, Comput. Phys. Commun. 181 (2010) 138, arXiv:0811.4169.

[48] P. Bechtle, O. Brein, S. Heinemeyer, G. Weiglein, K.E. Williams, HiggsBounds 2.0.0: confronting neutral and charged Higgs sector predictions with exclusion bounds from LEP and the tevatron, Comput. Phys. Commun. 182 (2011) 2605, arXiv:1102.1898.

[49] P. Bechtle, O. Brein, S. Heinemeyer, O. Stål, T. Stefaniak, G. Weiglein, et al., HiggsBounds − 4: improved tests of extended Higgs sectors against exclusion bounds from LEP, the tevatron and the LHC, Eur. Phys. J. C 74 (2014) 2693, arXiv:1311.0055.

[50] P. Bechtle, D. Dercks, S. Heinemeyer, T. Klingl, T. Stefaniak, G. Weiglein, et al., HiggsBounds-5: testing Higgs sectors in the LHC 13 TeV era, Eur. Phys. J. C 80 (2020) 1211, arXiv:2006.06007.

[51] H. Bahl, T. Biekötter, S. Heinemeyer, C. Li, S. Paasch, G. Weiglein, et al., HiggsTools: BSM scalar phenomenology with new versions of HiggsBounds and HiggsSignals, arXiv:2210.09332.

[52] P. Bechtle, S. Heinemeyer, O. Stål, T. Stefaniak, G. Weiglein, *HiggsSignals*: confronting arbitrary Higgs sectors with measurements at the tevatron and the LHC, Eur. Phys. J. C 74 (2014) 2711, arXiv:1305.1933.

[53] P. Bechtle, S. Heinemeyer, O. Stål, T. Stefaniak, G. Weiglein, Probing the standard model with Higgs signal rates from the tevatron, the LHC and a future ILC, J. High Energy Phys. 11 (2014) 039, arXiv:1403.1582.

[54] P. Bechtle, S. Heinemeyer, T. Klingl, T. Stefaniak, G. Weiglein, J. Wittbrodt, HiggsSignals-2: probing new physics with precision Higgs measurements in the LHC 13 TeV era, Eur. Phys. J. C 81 (2021) 145, arXiv:2012.09197.

[55] M. Muhlleitner, M.O.P. Sampaio, R. Santos, J. Wittbrodt, The N2HDM under theoretical and experimental scrutiny, J. High Energy Phys. 03 (2017) 094, arXiv:1612.01309.

[56] I. Engeln, M. Mühlleitner, J. Wittbrodt, N2HDECAY: Higgs boson decays in the different phases of the N2HDM, Comput. Phys. Commun. 234 (2019) 256, arXiv:1805.00966.

[57] J. Haller, A. Hoecker, R. Kogler, K. Mönig, T. Peiffer, J. Stelzer, Update of the global electroweak fit and constraints on two-Higgs-doublet models, Eur. Phys. J. C 78 (2018) 675, arXiv:1803.01853.

[58] W. Grimus, L. Lavoura, O.M. Ogreid, P. Osland, The oblique parameters in multi-Higgs-doublet models, Nucl. Phys. B 801 (2008) 81, arXiv:0802.4353.

[59] CDF collaboration, High-precision measurement of the W boson mass with the CDF II detector, Science 376 (2022) 170.

[60] Planck collaboration, Planck 2018 results. VI. Cosmological parameters, Astron. Astrophys. 641 (2020) A6, arXiv:1807.06209.

[61] G. Bélanger, F. Boudjema, A. Goudelis, A. Pukhov, B. Zaldivar, micrOMEGAs5.0: freeze-in, Comput. Phys. Commun. 231 (2018) 173, arXiv:1801.03509.

[62] T. Biekötter, P. Gabriel, M.O. Olea-Romacho, R. Santos, Direct detection of pseudo-Nambu-Goldstone dark matter in a two Higgs doublet plus singlet extension of the SM, J. High Energy Phys. 10 (2022) 126, arXiv:2207.04973.

[63] C. Gross, O. Lebedev, T. Toma, Cancellation mechanism for dark-matter–nucleon interaction, Phys. Rev. Lett. 119 (2017) 191801, arXiv:1708.02253.

[64] Y. Abe, Y. Hamada, T. Ohata, K. Suzuki, K. Yoshioka, TeV-scale majorogenesis, J. High Energy Phys. 07 (2020) 105, arXiv:2004.00599.

[65] Y. Abe, T. Toma, K. Tsumura, Pseudo-Nambu-Goldstone dark matter from gauged $U(1)_{B-L}$ symmetry, J. High Energy Phys. 05 (2020) 057, arXiv:2001.03954.

[66] N. Okada, D. Raut, Q. Shafi, Pseudo-Goldstone dark matter in a gauged $B-L$ extended standard model, Phys. Rev. D 103 (2021) 055024, arXiv:2001.05910.

[67] R.N. Mohapatra, N. Okada, Conformal B-L and pseudo-Goldstone dark matter, Phys. Rev. D 107 (2023) 095023, arXiv:2302.11072.

[68] D.-Y. Liu, C. Cai, X.-M. Jiang, Z.-H. Yu, H.-H. Zhang, Ultraviolet completion of pseudo-Nambu-Goldstone dark matter with a hidden U(1) gauge symmetry, J. High Energy Phys. 02 (2023) 104, arXiv:2208.06653.

[69] F.-A. Fortin, F.-M. De Rainville, M.-A. Gardner, M. Parizeau, C. Gagné, DEAP: evolutionary algorithms made easy, J. Mach. Learn. Res. 13 (2012) 2171.

[70] CMS collaboration, Search for dilepton resonances from decays of (pseudo)scalar bosons produced in association with a massive vector boson or top quark anti-top quark pair at $\sqrt{s} = 13$ TeV, Tech. Rep. CMS-PAS-EXO-21-018, 2022.

[71] S. Iguro, T. Kitahara, Y. Omura, Scrutinizing the 95–100 GeV di-tau excess in the top associated process, Eur. Phys. J. C 82 (2022) 1053, arXiv:2205.03187.

[72] ATLAS collaboration, Measurements of Higgs boson production cross-sections in the $H \to \tau^+\tau^-$ decay channel in pp collisions at $\sqrt{s} = 13$ TeV with the ATLAS detector, J. High Energy Phys. 08 (2022) 175, arXiv:2201.08269.

[73] G. Coloretti, A. Crivellin, S. Bhattacharya, B. Mellado, Searching for low-mass resonances decaying into W bosons, arXiv:2302.07276.

[74] ATLAS collaboration, Measurements of Higgs boson production by gluon-gluon fusion and vector-boson fusion using $H \to WW^* \to e\nu\mu\nu$ decays in pp collisions at $\sqrt{s} = 13$ TeV with the ATLAS detector, arXiv:2207.00338.

[75] CMS collaboration, Measurements of the Higgs boson production cross section and couplings in the W boson pair decay channel in proton-proton collisions at $\sqrt{s} = 13$ TeV, arXiv:2206.09466.

[76] W.G. Hollik, S. Liebler, G. Moortgat-Pick, S. Paßehr, G. Weiglein, Phenomenology of the inflation-inspired NMSSM at the electroweak scale, Eur. Phys. J. C 79 (2019) 75, arXiv:1809.07371.

[77] T. Biekötter, S. Heinemeyer, C. Muñoz, Precise prediction for the Higgs-Boson masses in the $\mu\nu$SSM with three right-handed neutrino superfields, Eur. Phys. J. C 79 (2019) 667, arXiv:1906.06173.

[78] K. Choi, S.H. Im, K.S. Jeong, C.B. Park, Light Higgs bosons in the general NMSSM, Eur. Phys. J. C 79 (2019) 956, arXiv:1906.03389.

[79] M. Cepeda, et al., Report from working group 2: Higgs physics at the HL-LHC and HE-LHC, CERN Yellow Rep. Monogr. 7 (2019) 221, arXiv:1902.00134.

[80] P. Bambade, et al., The international linear collider: a global project, arXiv:1903.01629.

[81] J. de Blas, et al., Higgs boson studies at future particle colliders, J. High Energy Phys. 01 (2020) 139, arXiv:1905.03764.

[82] P. Drechsel, G. Moortgat-Pick, G. Weiglein, Prospects for direct searches for light Higgs bosons at the ILC with 250 GeV, Eur. Phys. J. C 80 (2020) 922, arXiv:1801.09662.

[83] Y. Wang, M. Berggren, J. List, ILD benchmark: search for extra scalars produced in association with a Z boson at $\sqrt{s} = 500$ GeV, arXiv:2005.06265.